Bonding analysis for sterically uncongested, simple aurocarbons C_nAu_m

Patryk Zaleski-Ejgierd and Pekka Pyykkö

Abstract: The title series of simple model aurocarbons; CAu_4, C_2Au_2, C_2Au_4, C_2Au_6, and C_6Au_6 is investigated using Density Functional Theory with TPSS and B3LYP functionals and the second-order Møller-Plesset perturbation theory, with the latest Karlsruhe basis sets. The vibrational frequencies and the 0K thermodynamical properties are calculated. The bonding mechanism is also investigated. For C_2Au_n the calculated MP2 formation energy suggests increased stabilization with increasing *n*, due to the Au-Au aurophilic pair interactions.

Key words: aurocarbons, aurides, aurophilicity, metallophilicity, clusters, DFT, MP2

RECEIVED DATE

P. Zaleski-Ejgierd and P. Pyykkö.[1]
Department of Chemistry, University of Helsinki,
P.O. BOX 55 (A. I. Virtasen aukio 1), Helsinki
00014, Finland.

[1]Corresponding author:
(email: pekka.pyykko@helsinki.fi)

Introduction

Gold chemistry is fascinatingly rich. One of the conceptual tools in predicting new possible components is the chemical analogy between H and Au (or $-AuPR_3$). This was used to discuss CAu_4 (1) or $SiAu_4$ (2). Interestingly, the attempts to completely aurate methane resulted in the C_{4v} system $[HC(AuPR_3)_4]^+$ (3), theoretically found to have a large proton binding energy (4).

We furthermore note the existence of gold acetylides. A solid C_2Au_2 has been reported to be highly explosive (5). For other examples on gold-acetylide bonds, see Puddephatt (6). Recently Naumkin (7) considered the possibility of completely 'aurating' neopentane, $C(CH_3)_4$. The triple-bonded CAu^+, was predicted by Barysz and Pyykkö (8) and produced in the gas phase by Aquirre et al. (9). The dication CAu_2^{2+} was mass-spectroscopically observed by Gibson (10). Its electronic structure was interpreted by Pyykkö et al. (11) as $[Au{=}C{=}Au]^{2+}$, with bonding, similar to that of O=C=O. They also considered the D_{3h} CAu_3^+, observed by Gibson (10), and the C_2Au_2, that could be compared to either HCCH or $OCCO^{2-}$.

Against this background, we felt that a study of the aurated analogs of the simplest sp-, sp^2-, and sp^3-hybridized hydrocarbons would be interesting. The same, uncongested conformations as for their hydrocarbon analogs are given preferential treatment.

Computational Procedure

All the reported calculations were performed using the TURBOMOLE (v. 5.10) program package (12). Due to the expected presence of the aurophilic interactions the results were calculated with both Density Functional Theory (DFT) (13-14), and the second-order Møller-Plesset perturbation theory (MP2) (15) using the Resolution of Identity (RI) approximation, as implemented in TURBOMOLE (16). The recent, Karlsruhe quadruple-zeta (def2-QZVPP) basis sets were employed for all elements. In the case of gold, the 19-VE "small-core" Effective Core Potential (ECP) of Andrae *et al.* (17) was introduced to account for scalar relativistic effects. For carbon and nitrogen, we used the corresponding all-electron basis sets. The currently applied combination of bases and ECPs was found to be suitable for calculations involving weak Au-Au interactions (18).

Fig. 1. The aurocarbons, including the isoelectronic $[AuCNAu]^+$. The Au-Au and Au'-Au' notation denote the shorter and longer aurophilic distances respectively.

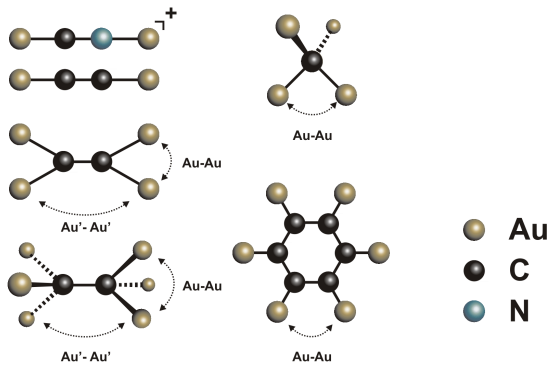

Table 1. The calculated bond distances for aurocarbons in Fig. 1. All values in pm.

Case	Method	C-C	Au-C	Au-Au	Au'-Au'
CAu_4	B3LYP	---	198.74	324.55	---
	TPSS	---	196.54	320.94	---
	RI-MP2	---	190.21	310.62	---
C_2Au_2	B3LYP	121.50	191.87	---	---
	TPSS	122.49	190.13	---	---
	RI-MP2	122.51	184.99	---	---
C_2Au_4	B3LYP	131.60	199.13	326.50	359.88
	TPSS	132.99	196.78	325.59	354.06
	RI-MP2	133.14	189.92	314.26	346.48
C_2Au_6	B3LYP	147.94	203.32	317.38	372.35
	TPSS	148.83	200.31	314.12	365.67
	RI-MP2	146.66	193.15	304.66	353.19
	HF	148.57	207.99	322.15	382.96
C_6Au_6	B3LYP	139.68	200.07	339.75	---
	TPSS	140.13	197.85	337.98	---
	RI-MP2	138.84	190.99	329.80	---

The vibrational analysis was performed within the harmonic approximation at both DFT and RIMP2 levels of theory. The DFT/TPSS results are depicted in Fig. 2.

In case of the DFT approach, two exchange-correlation functionals were used, namely: the B3LYP hybrid functional (19-20) and the meta-generalized-gradient-approximation TPSS functional (21). We used the small-size grid (434 gridpoints) for numerical integration.

For the RI-assisted MP2, the corresponding auxiliary basis sets were applied (22), and all the explicitly treated electrons were correlated.

The spin-orbit interactions were neglected. For an s-element such as gold, and closed-shell species, this is expected to be reasonable.

The partial atomic charges were estimated using the Mulliken population analysis scheme, as implemented in the TURBOMOLE package. The Molecular Orbital (MO) contours were generated using Molden (v. 4.6) package (23).

Table 2. The partial Mulliken charges, δ, for structures considered in Fig. 1.

Case	Method	δC	δAu(C) / δAu(N)	δN
$[AuCNAu]^+$	B3LYP	-0.25	+0.79 / +0.79	-0.30
	TPSS	-0.27	+0.76 / +0.83	-0.33
	HF	-0.30	+0.88 / +0.92	-0.50
CAu_4	B3LYP	-1.27	+0.32 / ---	---
	TPSS	-1.30	+0.33 / ---	---
	HF	-1.52	+0.38 / ---	---
C_2Au_2	B3LYP	-0.31	+0.31 / ---	---
	TPSS	-0.34	+0.34 / ---	---
	HF	-0.47	+0.47 / ---	---
C_2Au_6	B3LYP	-1.31	+0.44 / ---	---
	TPSS	-1.43	+0.48 / ---	---
	HF	-1.43	+0.48 / ---	---
C_6Au_6	B3LYP	-0.61	+0.61 / ---	---
	TPSS	-0.64	+0.64 / ---	---
	HF	-0.42	+0.42 / ---	---

Each of the six model compounds was optimized with the specific symmetry constrains: CAu_4 (C_1, effectively T_d), C_2Au_2 (C_{2v}, effectively $D_{\infty h}$), C_2Au_4 (D_{2h}), C_2Au_6 (D_{3d}), C_6Au_6 (D_{6h}) and $[CNAu_2]^+$ (C_{2v}, effectively $C_{\infty v}$). The resulting equilibrium structures were subjected to numerical vibration analysis. We did not find any imaginary frequencies.

Results and Discussion

The geometry trends

We first note that although the investigated structures exhibit only real vibrational frequencies, the presented structures do not necessarily correspond to the global energy minima. It is possible that planar structures may be favored, for instance 2D 'flakes' are known to be exceptionally stable up to a certain number of gold atoms, depending on the electrical charge. (24-25).

In this work we did not try to identify such energetically lowest isomers, instead we rather investigated the general trends of a new family of aurocarbons. The digold monocyanide cation, $[AuCNAu]^+$, was added as a potential isoelectronic species to C_2Au_2 for cation experiments.

The calculated equilibrium structures are depicted in Fig. 1, while the corresponding geometrical parameters are presented in Table 1.

The DFT results obtained with the two different functionals (B3LYP and TPSS) agree. The average C-C bond length difference is ~0.93pm, and the Au-C difference is ~2.15pm. The discrepancy rises with the saturation of C-C bond.

The RIMP2 and DFT structures differ slightly. Two clear trends can be observed. In case of the Au-C and Au-Au/Au'-Au' bonds, the RIMP2 distances are always the shortest, followed by TPSS and B3LYP. The opposite trend is observed in case of the C-C bond, with the notable exception of C_6Au_6.

The calculated Au-C and C-C bond lengths in C_2Au_2 are in good agreement with the experimental data obtained by Puddephatt et al. for species containing similar bonding patterns (26).

The C-C distances in the C_2Au_2, C_2Au_4 and C_2Au_6 are closely comparable with the corresponding hydrocarbons,

Fig. 2. The DFT/TPSS harmonic frequency spectra [cm^{-1}] calculated for the family of aurocarbons.

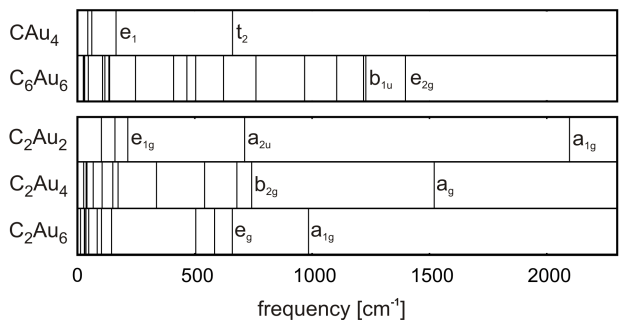

Fig. 3. (Color online) The 37 highest occupied Kohn–Sham (TPSS) molecular orbitals of C_2Au_6 (D_{3d}). The LUMO orbital energy is -0.130 a.u., resulting in a gap of 0.048 a.u. or +1.31eV. (HO-n stands for HOMO-n).

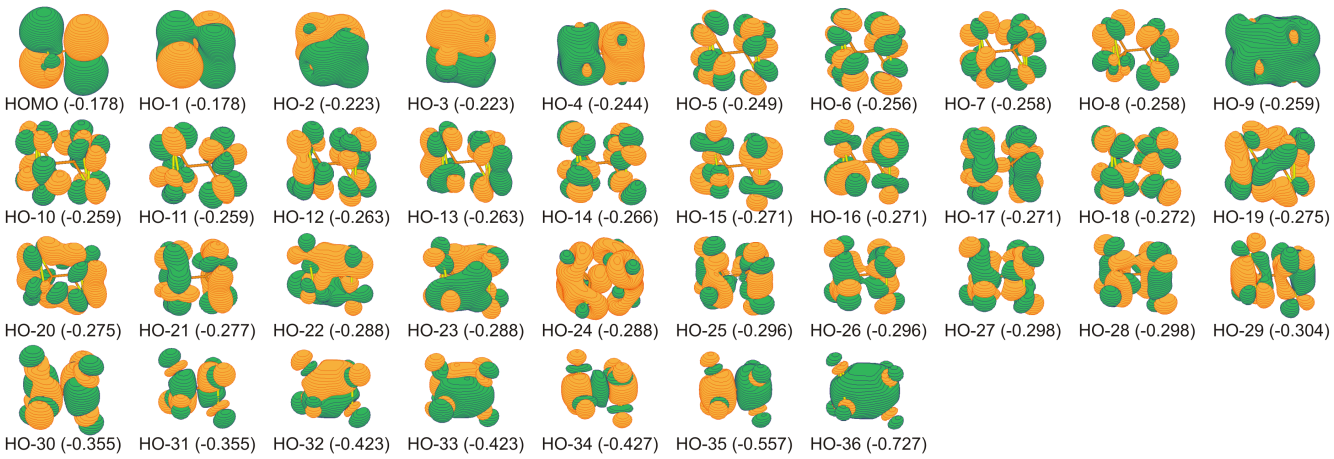

suggesting analogous bonding. Interestingly, the C-C bond in C_2Au_6 is shorter than in C_2H_6 by ≤10pm.

The Au-C distance varies from one molecule to the other by up to ~12pm and depends strongly on the type of the C-C bond. It lengthens with the level of substitution (or shortens with the hybridization as sp < sp^2 < sp^3, like the C-H bonds do).

While the Au'-Au' distances only yield weak aurophilic interactions, the Au-Au distances are expected to have stronger ones. The Au-C-C angles remain practically constant for different methods: 124.18º, 124.96º and 124.17º for C_2Au_4 and 115.12º, 115.68º and 114.40º for C_2Au_6 at the B3LYP, TPSS and RIMP2 level of theory respectively.

Vibrations

The harmonic frequencies were calculated at three levels of theory: DFT with the B3LYP and the TPSS exchange-correlation functionals and with the RIMP2.

The TPSS frequencies are depicted in Fig. 2. The B3LYP results are similar, while the RIMP2 tend to give slightly higher values. The fact can be related to the M-C overbinding typical for MP2 method. The highest frequencies correspond to C-C stretch, while the lowest, to the out-of-plane deformations and the rotations with respect to the C-C axis. In the unlikely case of quantum dynamics for the gold nuclear motions, six gold atoms could still occupy the same special quantum state, with nuclear spin M_I from -5/2 to +5/2 (27).

Thermochemistry

The thermochemical analysis for a series of reactions listed in Table 3 was performed with respect to the isolated Au_2 and the C(^3P_j) atoms. The CAu_4 and C_2Au_2 formation energy from pure elements (Table 3, cases 1-2) was found to be strongly negative for all methods. The energy of Au_2 addition in a C_2Au_2, C_2Au_4 series (cases 3-4) varies with method. It remains negative for TPSS and RIMP2 but changes sign in case of B3LYP results. The trimerization energy of C_2Au_2 units (case 5) is strongly exothermic. Since the accuracy of such estimate might be questionable, we applied an isodesmic approach (Table 3, cases 6-10) to make sure that the broken chemical bonds are of the same type as the type of bonds formed in the reaction. The DFT formation energy calculated per one Au-C bond is approximately constant for a given functional. Interestingly, the same energy calculated at RIMP2 level decreases systematically in the C_2Au_n (n=2, 4, 6) series and became thermo-neutral for C_2Au_6, most likely due to aurophilic stabilization. It is known that this attraction is exaggerated at the MP2 level (28).

Bonding

The TPSS Kohn-Sham orbitals are given as Supplementary Information. They all correspond to the combinations, expected from the existing C-C and Au-C local bonding orbitals. A fair amount of hybridization is also seen in the Au 5d band. An example on C_2Au_6 is depicted in Fig. 3. The simplest way to understand the bonding orbitals of C_2Au_6 (D_{3d}) in Fig. 3 is to classify the bonding orbitals HOMO to HOMO-4, and HOMO-9, as the e_g (2x), t_{1u} (3x), and a_{1g} combinations of the six Au-C local bonding orbitals under octahedral, quasi-O_h symmetry. The corresponding nodal structures are conspicuous in Fig. 3. The Mulliken charges are shown in Table 2. The C atoms are negative and the Au atoms positive.

Possible extensions

The present ideas can be extended by considering ionic, isoelectronic analogs (BAu_4^-, CAu_4, NAu_4^+ (1)) or by introducing other rows of the Periodic Table (CAu_4, $SiAu_4$, etc.). Another possibility is to replace the plain –Au by –$AuPR_3$ (4). The latter proposition is more realistic for bulk compounds. Many such monocentric compounds already exist while the bicentric (C_2Au_6, etc.) gold compounds are more rare.

Table 3. The thermochemical cycles.

Case	Total ΔE (kJ mol^{-1})			ΔE per Au-C pair (kJ mol^{-1})		
	B3LYP	TPSS	RIMP2	B3LYP	TPSS	RIMP2
1. $C + 2Au_2 \rightarrow CAu_4$	-545	-763	-829	-	-	-
2. $2C + Au_2 \rightarrow C_2Au_2$	-1068	-1168	-1189	-		-
3. $C_2Au_2 + Au_2 \rightarrow C_2Au_4$	-58	-174	-229	-	-	-
4. $C_2Au_4 + Au_2 \rightarrow C_2Au_6$	+24	-105	-254	-	-	-
5. $3C_2Au_2 \rightarrow C_6Au_6$	-512	-583	-850	-	-	-
6. $C_2H_2 + Au_2 \rightarrow C_2Au_2 + H_2$	+154	+55	+107	+77	+27	+54
7. $C_2H_4 + 2Au_2 \rightarrow C_2Au_4 + 2H_2$	+303	+88	+78	+76	+22	+19
8. $C_2H_6 + 3Au_2 \rightarrow C_2Au_6 + 3H_2$	+486	+144	-3	+81	+23	-0.5
9. $C_6H_6 + 3Au_2 \rightarrow C_6Au_6 + 3H_2$	+581	+242	+143	+97	+40	+24
10. $CH_4 + 2Au_2 \rightarrow CAu_4 + 2H_2$	+291	+70	+43	+73	+17	+11

Conclusions

We have considered the H→Au analogs of the simplest hydrocarbons CH_4, C_2H_2, C_2H_4, C_2H_6, and C_6H_6. All are found to be local minima, but their Au-C bonding energies are smaller than the corresponding C-H ones.

The C_2Au_6 system possesses increased stability at MP2 level and has in its D_{3d} structure altogether twelve aurophilic Au^I-Au^I attractions.

Acknowledgement

We belong to the Finnish Centre of Excellence (CoE) in Computational Molecular Science (CMS, 2006–2011). The Magnus Ehrnrooth Foundation is acknowledged for providing financial support and the Centre of Scientific Computing (CSC) Espoo, Finland for providing computer resources.

References

1. P. Pyykkö, and Y.-F. Zhao. Chem. Phys. Lett., **177**, 103 (1991).
2. B. Kiran, X. Li, H.-J. Zhai, L.-F. Cui, and L.-S. Wang. Angew. Chem. Int. Ed., **43**, 2125 (2004).
3. H. Schmidbaur, F. P. Gabbaï, A. Schier, and J. Riede. Organometallics, **14**, 4969 (1995)
4. P. Pyykkö, and T. Tamm. Organometallics, **17**, 4842 (1998).
5. M.C. Sneed, J.L. Maynard, and R.C. Brasted. Comprehensive Inorganic Chemistry, Vol. 2, D. van Nostrand Co., Inc., 238 (1954).
6. R. J. Puddephatt. Chem. Soc. Rev. **37**, 2012 (2008).
7. F. Naumkin. Phys. Chem. Chem. Phys., **8**, 2539 (2006).
8. M. Barysz, and P. Pyykkö. Chem. Phys. Lett. **285**, 398 (1998).
9. F. Aguirre, J. Husband, C. J. Thompson, and R. B. Metz. Chem. Phys. Lett. **318**, 466 (2000).
10. J. K. Gibson. J. Vac. Sci. Technol. A. **16**, 653 (1998).
11. P. Pyykkö, M. Patzschke, and J. Suurpere. Chem. Phys. Lett. **381**, 45 (2003)
12. R. Ahlrichs, M. Bär, M. Häser, H. Horn, and C. Kölmel. Chem. Phys. Lett. **162**, 165 (1989).
13. P. Hohenberg and W. Kohn. Phys. Rev., **136**, 864 (1964).
14. W. Kohn and L. J. Sham. Phys. Rev., **140**, 1133 (1965).
15. Møller C., and Plesset M.S. Phys. Rev., **46**, 618 (1934).
16. F. Weigend, A. Köhn, and C. Hättig. J. Chem. Phys., **116**, 3175 (2001).
17. D. Andrae, U. Häußermann, M. Dolg, H. Stoll, and H. Preuß. Theor. Chim. Acta **77**, 129 (1990).
18. P. Pyykkö, and P. Zaleski-Ejgierd. J. Chem. Phys., **128**, 124309 (2008).
19. A. D. Becke. J. Chem. Phys., **98,** 1372 (1993).
20. P. J. Stephens, F. J. Devlin, C. F. Chabalowski, M. J. Frisch. J. Phys. Chem., **98**, 11623 (1994).
21. J. Tao, J. P. Perdew, V. N. Staroverov, and G. E. Scuseria. Phys. Rev. Lett., **91**, 146401 (2003).
22. F. Weigend, M. Häser, H. Patzelt, and R. Ahlrichs. Chem. Phys. Lett., **294**, 143 (1998).
23. G. Schaftenaar, and J. H. Noordik. J. Comput.-Aided Mol. Design, **14**, 123 (2000).
24. H. Häkkinen. Chem. Soc. Rev., **37**, 1847 (2008).
25. P. Pyykkö. Chem. Soc. Rev., **37**, 1967 (2008).
26. N. C. Payne, R. Ramachandran, and R. J. Puddephatt. Can. J. Chem. **73**, 6 (1995).
27. J. Autschbach, B. A. Hess, M. P. Johansson, J. Neugebauer, M. Patzschke, P. Pyykkö, M. Reiher, and D. Sundholm. Phys. Chem. Chem. Phys., **6**, 11 (2004).
28. P. Pyykkö, N. Runeberg and F. Mendizabal. Chem. Eur. J. **3**, 1451 (1997).